JCAMECH

Vol. 47, No. 1, June 2016, pp 35-44
DOI: 10.22059/jcamech.2016.59253

A finite elements study on the role of primary cilia in sensing mechanical stimuli to cells by calculating their response to the fluid flow

Amirhossein Abbasszadeh Rad, Bahman Vahidi*

[1]*Division of Biomedical Engineering, Department of Life Science Engineering, Faculty of New Sciences and Technologies, University of Tehran, Tehran, Iran*

Received: 7 Feb. 2016 , Accepted: 30 Apr. 2016

Abstract

The primary cilium which is an organelle in nearly every cell in the vertebrate body extends out of the cell surface like an antenna and is known as cell sensor of mechanical and chemical stimuli. In previous numerical simulations, researchers modeled this organelle as a cantilevered beam attached to the cell surface. In the present study, however, we present a novel model that accommodates for both pivoting and bending of primary cilium in response to the fluid flow. In this model, primary cilium is attached to the cell using a thin elastic layer. This layer, which comprises the bottom boundary of the cilium, provides the possibility of pivoting of the cilium around its base so that we are able to analyze the other part of ciliary response to the fluid flow. In this study, we have used finite element method and fluid-structure interaction techniques to simulate the problem. Domains of solid cilium and the surrounding fluid were meshed using triangular elements. The governing equations in this problem were fully coupled and were solved by the direct method. Graphs of maximum stress in the cilium base versus elastic constant of the thin layer depict two different trends. By scrutinizing colored plots of stress distribution in the cilium base it is construed that these trends represent two different mechanisms in ciliary deformation due to the flow of the fluid. In case of low elasticity constants, for which attachment of the cilium to the cell is soft, pivoting mechanism is essential, while in case of harder attachments, bending mechanism dominates.

Keywords:

Primary Cilium, Thin Elastic Layer, Mechanosensation, Fluid-Structure Interaction, Cell Mechanics

1. Introduction

Cilia are extrusions that protrude from cell body into the extracellular matrix. They are divided into two types of motile cilia and non-motile or primary cilia,

* Corresponding Author. Tel.: +98 21 61118407
Email Address: bahman.vahidi@ut.ac.ir

the latter of which is the subject of this study. Primary cilia are organelles that are present in nearly every cell in the body. Primary cilia can sense the fluid flow around the cells by being deflected. Cells typically have one primary cilium in a point during their cell cycle [1]. Primary cilia are studied mainly because of their role in poly cystic kidney disease and they have been shown to have a key role in sensing fluid shear stress [2]. They are also important in differentiation of mesenchymal stem cells to osteocytes in response to periodic fluid flow [3, 4]. Hence, this sensory organelle constitutes a growing area of investigation in tissue engineering.

Primary cilia have been investigated in other kinds of cells. Their essential role in differentiation of human adipose-derived stem cells hASC have been recently reported [5]. These cells exhibit mechanosensitivity in response to different kinds of mechanical stimuli. For example, cyclic tensile strain exerted to hASC promotes their osteogenesis and cell-mediated calcium accretion [6-8].

Natural cell function includes a complex set of cell processes that interact with each other. Inputs of those processes are external stimuli exerted to the cell, among which are physical stimuli such as temperature, pressure, tensile stress and fluid flow. What matters to the present study is that primary cilium has been described as an organelle involved in sensing the fluid flow [9].

Cilium structure is constructed of more than 650 proteins [10] with different functionalities such as temperature sensing proteins [11] and ion channels [12]. In 2001 researchers have first found that primary cilia in epithelial kidney cells can produce intracellular calcium in response to fluid flow [13]. Since then a protein complex which consists of polycystin-1 and polycystin-2 were found to be concentrated on cilium [14]. This protein was suggested to play the role of a calcium channel in ciliary membrane [15] and initiate calcium intake by bending of the cilium. Malfunction of either polycystine-1 or polycystin-2 results in polycystic kidney disease.

Upon flow of fluid over the cell surface, primary cilium bends and the surrounding membrane experiences strain resulting in activation of ion channels and transfer of special kinds of ions. Thus, primary cilium is able to transduce mechanical stimuli to ion signals and to make the cell somehow sense the surrounding fluid flow.

Until now different groups of researchers have modelled primary cilium in order to simulate its response to different kinds of mechanical stimuli such as shear stress due to fluid flow, and also tensile strain exerted from extra cellular matrix. They have hypothesized the cilium as a cantilevered beam with fixed constraint to the cell which is merely free to bend. Recently, there have been some evidence which casts doubts on this hypothesis, showing that primary cilium is free to change direction. In this study we try to address the question that whether or not this hypothesis is of any consequence by developing a model which accommodates for both pivoting and bending of primary cilium in response to the fluid flow. In this model, the primary cilium is attached to the cell surface through a thin layer with elastic properties. The model is solved using finite element methods and fluid-structure interaction techniques. Triangular elements are used to mesh the domains of solid cilium and the surrounding fluid. Here we briefly describe work of others that is immediately related to that of ours.

Mathieu et al. investigated ciliary response to tensile strain [16]. They used finite element analysis (FEA) to determine strains occurring within the ciliary membrane in response to 10% tensile strain applied parallel, or perpendicular, to cilia orientation. They calculated principal tensile strains in both human adipose-derived stem cells (hASC) and ciliary membranes, and determined the magnitude and location of maximum principal tensile strain. They modeled cilia of different lengths and compared the results of linear elastic model with those of hyper elastic model and concluded that cilium orientation might be more important than cilium length in determining sensitivity of hASC to tensile strain.

Rydholm et al. focused on the mechanics of cilium bending and the resulting calcium signal [9]. They observed that the bending of cilia is fast compared with the initiation of calcium increase within cells. By mathematical modeling of cilium and surrounding membrane they deduced the relation between bending and membrane stress. The results showed a delay in stress buildup that was similar to the delay in calcium signal. Their results thus indicated that the delay in calcium response upon cilia bending is caused by mechanical properties of the cell membrane.

Battle et al. found that, on manipulation with an optical trap, cilia deflect by bending along their length and pivoting around an effective hinge located below the basal body [17]. They closely examined the relaxation curves of cilia from the bend and relax experiments, and found systematic deviations from single-exponential time dependence. According to them, those curves could typically be better fit by a sum of two exponentials. Initial fast relaxation occurs on the order of hundreds of milliseconds followed by a slower reorientation of the cilium to its resting

position normal to the cell surface. Considering this evidence, they suggested a viscoelastically hinged rather than a rigidly clamped boundary condition for ciliary deflection.

Khayyeri et al. used a finite element computational approach to model not only primary cilium but also nucleus, cytoplasm, cortex, microtubules and actin bundles. Their results indicate that primary cilium deflection under fluid flow stimulation transmits mechanical strain primarily to other essential organelles in the cytoplasm, such as the Golgi complex, that regulate cells' mechanoresponse. Their simulations further suggest that cell mechanosensitivity can be altered by targeting primary cilium length and rigidity. According to them, their findings suggest that the degree of mechanosensitive response of ciliated cells depends partly on the mechanics of the primary cilium, which regulates the mechanical stimuli transduced to nucleus and to specific locations of the cytoplasm where the Golgi apparatus is located [18]. In their model, a kind of constraint named tie constraint was used to attach the cilium to the cell.

In most previous numerical studies, cilium was modeled as a cantilevered beam so that pivoting around the above-mentioned hinge was not taken into account. In the present study, a boundary condition other than the fixed and rigid one is applied between cilium base and cell surface so that the cilium not only bends in response to fluid flow, but also changes direction.

2. Materials and Methods

We used a finite element model containing Fluid-Structure Interactions. A cilium which extends from cell surface is simulated in COMSOL Multiphysics (Version 4.4). This cilium is immersed in the fluid surrounding the cell and is subject to shear stress due to flow of the fluid. An approximate 2D model is used in this study which is a narrow strip submerged in a flow channel. This strip, which resembles primary cilium, is a rectangle 2.7 to 7 micrometers long and 200 nanometers wide—just the same as reports of the cilium diameter[9, 16]. On top of this rectangle, there is a half circle which models head of the cilium while at the bottom of it, fillets of radii 0.03 to 0.05 micrometers are added. Height of the channel is 50 micrometers in this study. Other parameters and values used in the simulation are listed in Table .

Table 1 Parameters and values used in the model

Parameter	Definition	Value	Reference
ρ	Density of fluid	1000 kg/m^3	[9]
μ	viscosity of the fluid	0.000697 Pa.s	[9]
τ	Shear stress in flow field	0.02-0.06 Pa	[9]
E	Young modulus of solid	178000 Pa	[9]
ν	Poisson's ratio	0.33	[9]
K	Spring constant	>10000 N/m	-

Governing equations of fluid and solid domains were solved simultaneously so these equations are considered fully coupled in our solving method.

2.1. *Boundary Conditions*

As shown in Figure , inlet velocity of the fluid linearly increases from zero at the bottom of the channel to a specified value at the top of it. There is no-slip boundary condition at the bottom and a sliding wall at the top of the channel. This way, linear profile of velocity at the inlet will be kept nearly unchanged and a laminar flow will develop throughout the channel, in which an almost constant shear stress exists. Outlet pressure of the fluid is set to zero.

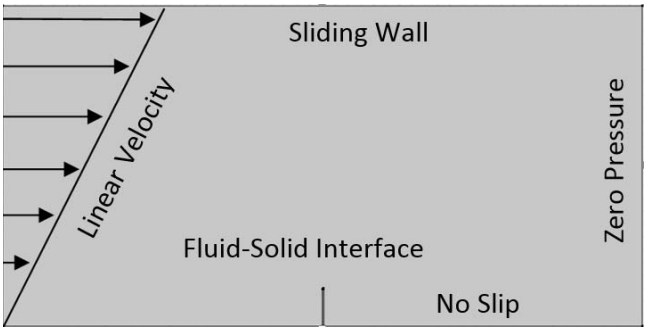

Figure 1 Boundary conditions

Despite previous studies, in which a primary cilium was attached to the cell surface by fixed constraints, in our model, the cilium is connected to the

bottom wall of the channel through a thin elastic layer called spring foundation. This layer, which is of infinitesimal thickness, can have different values of stiffness and damping coefficient.

2.2. *Governing Equations*

The governing equations for a 2D unsteady incompressible laminar flow are the continuity and Navier-Stokes equations[19].

Continuity:

$$\rho \nabla . u_{fluid} = 0 \tag{1}$$

Navier-Stokes:

$$\rho \frac{\partial u_{fluid}}{\partial t} + \rho \left(u_{fluid} . \nabla\right) u_{fluid} = \nabla . [-pI + \mu \left(\nabla u_{fluid} + \left(\nabla u_{fluid}\right)^T\right] + F \tag{2}$$

where ρ is fluid density, u_{fluid} is fluid velocity, t is time, p is pressure, I is unit tensor, μ is dynamic viscosity and F is volume force.

No-slip condition which is applied to walls of the duct is:

$$u_{fluid} = 0 \tag{3}$$

for the lower wall and:

$$u_{fluid} = U \tag{4}$$

for the upper wall where U is the velocity of the upper wall of the channel.

Equations governing fluid-solid interface boundary are [20]:

$$u_{fluid} = u_w \tag{5}$$

$$u_w = \frac{\partial u_{solid}}{\partial t} \tag{6}$$

$$\sigma . n = \Gamma . n \tag{7}$$

where u_w is wall velocity, u_{solid} is solid displacement, σ is stress tensor of solid, n is normal vector and Γ is the stress tensor for Newtonian fluid:

$$\Gamma = [-pI + \mu \left(\nabla u_{fluid} + \left(\nabla u_{fluid}\right)^T\right] \tag{8}$$

Equation governing the solid domain is that of isotropic linear elastic material [21]:

$$\rho \frac{\partial^2 u_{solid}}{\partial t^2} - \nabla . \sigma = (I + \nabla u_{solid}) v \tag{9}$$

where v is Poisson's ratio.

Boundary condition at the base of the cilium using fixed constraint or cantilever is [22]:

$$u_{solid} = 0 \tag{10}$$

Upon using spring foundation, this boundary condition becomes [23]:

$$\sigma . n = -\mathrm{k}(u_{solid} - u_0) \tag{11}$$

where u_0 is the initial value of u_{solid} and k is spring constant. No damping is included in this foundation.

Shear stress in fluid domain is obtained using the following formula for Newtonian fluids:

$$\tau = \mu \frac{U}{H} \tag{12}$$

where H is the height of the channel.

2.3. *Grid*

An unstructured mesh was generated for this model using the "Free Triangular" node of the software. Fluid and solid domains was divided into approximately 40000 and 3500 triangular elements, respectively. This kind of element is the default element type for most physics within COMSOL Multiphysics and is most common in unstructured grids. A triangular surface mesh is always quick and easy to create. Any geometry, regardless of shape or topology, can be meshed with triangular elements. Since this model consists of a cilium with round fillets within a rectangular duct, we chose to use an unstructured grid with triangular elements so that we could mesh these two geometrically dissimilar domains without much effort. Resolution of narrow regions was set to 10 so that small width of the cilium can be meshed appropriately. To inspect mesh independency of the results, we used three different mesh structures and compared the results in a problem with the following parameters:

Cilium Length:	6 μm
Shear Stress in Fluid Domain:	0.04 Pa
Fillet Radius:	0.05 μm
Spring Constant	9×10^5 N/m

Figure 2 shows our primary grid used in this study. The left part of the figure shows the entire domain while the right part magnifies the base of the cilium.

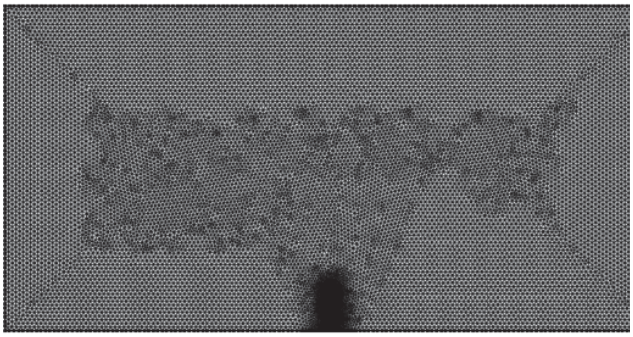

Figure 2 Numerical mesh. (Left) entire domain; (Right) around cilium base.

We solved the problem with the above mesh and two other mesh structures to obtain the maximum stress and the average von Mises stress in the cilium. We also solved the problem for different element sizes. Deviation of the results from average was less than 15% for maximum stress and less than 5.6% for the average von Mises stress.

2.4. *Convergence*

This simulation was performed using iterative methods in which convergence is a matter of concern. For this reason we include convergence plots of our simulation here to show that the curves are acceptably decreasing functions.

Figure 3 shows the convergence plots of two different simulated cilia. It is shown that in the cantilevered model, convergence was reached in just 11 iterations, while in the model containing spring foundation, in 24 iterations the solution converged. It is because in the latter model the cilium is more flexible so it substantially deforms, which results in more extensive change in the fluid domain. That is why the solver has to repeat the calculations more times in order to reach a converged solution from the same initial conditions. Nevertheless, convergence plots have the same descending trends in both cases. Please note that the convergence plot shown in Figure 3 is that of a model with spring constant 10000 N/m, which is too low. In other cases with stiffer spring foundations, and therefore less deformations, convergence surely improves.

3. Results and Discussion

Since stretch activated ion channels are present in the ciliary membrane, maximum strain in the external layer of the cilium is what we should calculate. Nevertheless, stress and strain are linearly dependent to each other because we used linear elastic material in our model. That is why we just calculate maximum von mises stresses in various problems to understand how a change in a specific parameter affects the maximum stress.

Figure 4 depicts the flow field in the channel and the stress field in a bent cantilevered cilium of length 6 micrometers with fillets of radius 0.04 micrometers, which is subject to 0.04 Pa shear stress exerted from fluid.

The color legend on the right is for the velocity field and the other color legend is for the stress field. We substituted the fixed constraint boundary condition at the base of the cilium with a spring foundation and solved the problem for different values of spring constant. Results are listed in Table 2 and shown in Figure 5.

The graph shown in Figure 5 consists of three segments. The horizontal segment suggests that if spring constant approaches infinity, the result approaches that of cantilevered beam. In this problem spring constants more than 20×10^6 N/m make the primary cilium like a cantilevered beam so that further increase in the spring constant has no effect on the results.

Now we try to delve into this graph by magnifying the transition segment where the horizontal segment joins the vertical segment as shown in Figure 6.

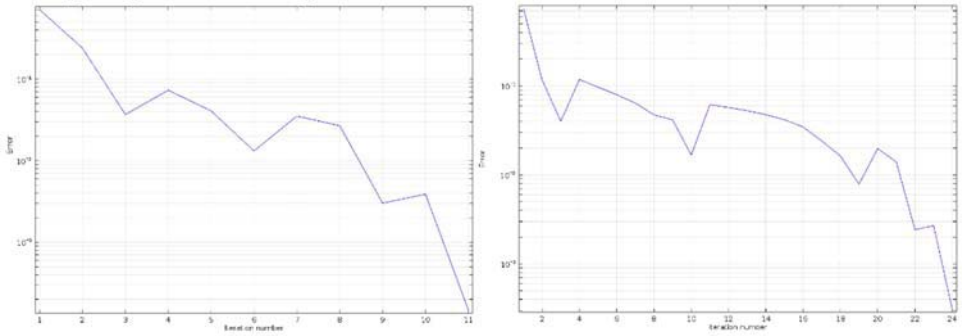

Figure 3 convergence plot. Left: a cantilevered cilium. Right: a cilium with spring foundation of spring constant 10000 N/m

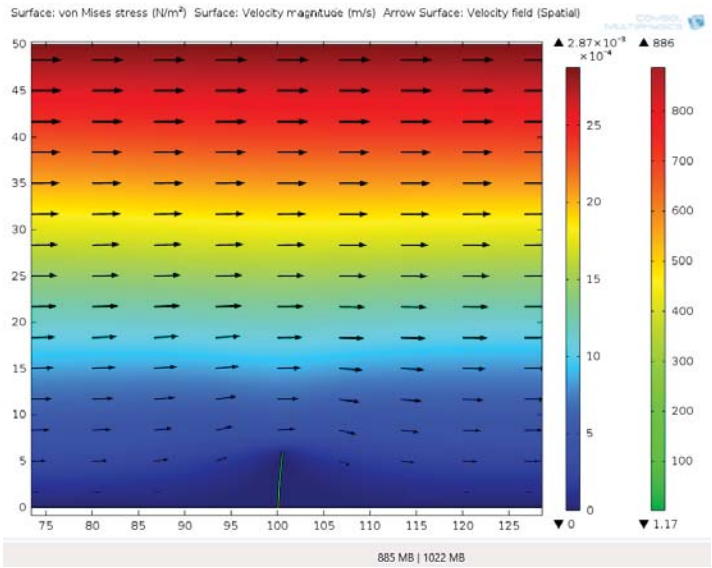

Figure 4 stress field in the cilium and the velocity field in the fluid domain

Table 2 data of maximum stress for different value of spring constant of the spring foundation

spring constant (N/m)	σ max (Pa)	spring constant (N/m)	σ max (Pa)
fixed constraint	886	900000	1039
100000000	888	800000	1055
10000000	904	700000	1100
9000000	906	600000	1156
8000000	909	500000	1228
7000000	912	400000	1324
6000000	916	300000	1462
5000000	922	200000	1678
4000000	930	150000	1846
3000000	943	100000	2304
2000000	967	60000	3536
1600000	984	30000	5721
1300000	1001	10000	8762
1000000	1027		

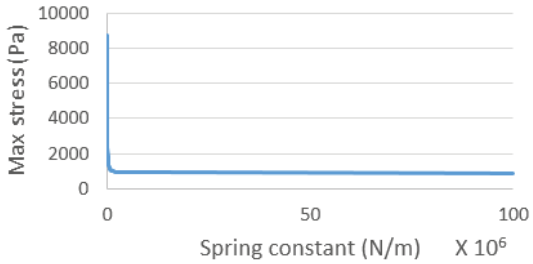

Figure 5 Maximum stress in the deformed cilium due to the fluid flow vs. spring constant of the spring foundation

This figure suggests that there is a logarithmic relationship between Max stress and spring constant so we redraw the graph in a logarithmic scale in Figure 7.

This graph consists of two almost linear segments with different slopes. The linearity of these curves proves that maximum stress has a logarithmic relationship with spring constant, but logarithms to two different bases nonetheless. This fact suggests that there might be two different mechanisms by which an increase in spring constant results in a decrease in the maximum stress. In this specific example spring constant of $8x10^5$ N/m is the transition point between these two mechanisms.

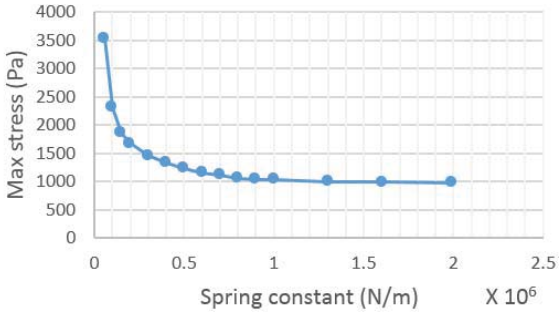

Figure 6 Transition segment of maximum stress vs. spring constant

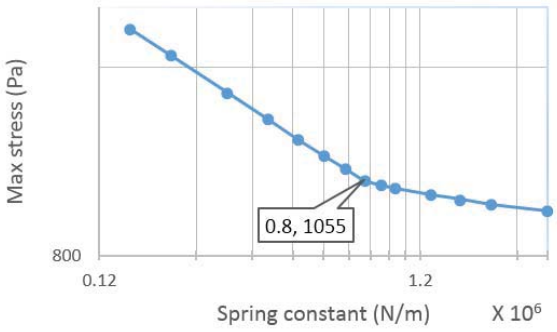

Figure 7 Log-log plot of maximum stress vs. spring constant for a cilium with fillets of radius 0.04 μm

Taking a look at colored plots of stress distribution in the cilium base reveals that in the cantilevered model maximum stress occurs just at the top of the fillets. In the models with spring foundation, however, regions of maximum stress have come closer to the fillets. This is shown in Figure 8

Comparing these plots and considering the above-mentioned logarithmic graph shown in Figure 7, it can be construed that there are two modes of deflection of primary cilium in response to the force exerted from fluid flow; bending and pivoting.

In bending mode, the maximum stress occurs around the base at the top of the fillets. This mode is dominant when there is a stiff attachment between the cilium and the cell surface. In this example the criterion for stiffness of the attachment is the spring constants higher than $8x10^5$ N/m. This value for spring constant is where the slope of the curve suddenly changes in the logarithmic graph of maximum stress versus spring constant.

For spring constants lower than $8x10^5$ N/m the pivoting mode, which is easily discernible in Figure 8-right is dominant. Please note that the plot in Figure 8-right is a gross exaggeration just to depict the pivoting of the cilium around an imaginary hinge located at its base, so the numerical values in this figure are not valid.

Now the question arises as to what factors determine the transition point between these two mechanisms of cilium deflection. It is seen that by decreasing the spring constant of the foundation, which results in a softer cilium to cell attachment, the location of the maximum stress tends to move into the fillets and the pivoting mode tends to dominate. That is why we conjectured that the radius of fillets is an important factor in the value of spring constant for which the transition between deflection modes occurs.

In order to check whether this conjecture is true, we repeated the simulations for cilia with fillets of radii 0.05 and 0.03 micrometers. Results are summarized in Figure 9.

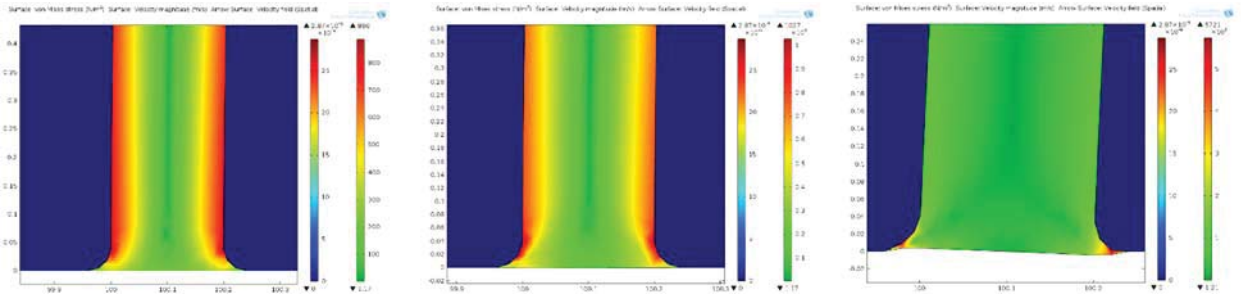

Figure 8 Stress distribution in the bases of primary cilia of length 6 μm with fillets of radius 0.04 μm subject to 0.04 Pa shear stress of fluid flow. Left: Cantilevered model. Middle: Spring foundation model with spring constant of 106 N/m. Right: spring foundation model with spring constant of 3x104 N/m

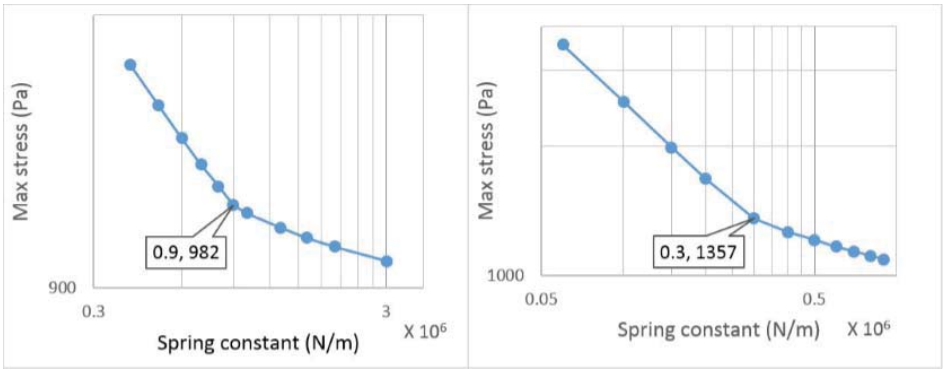

Figure 9 Log-log plot of maximum stress vs. spring constant for cilia with fillets of radii 0.05 μm (left), and 0.03 μm (right)

Results show that decreasing fillet radius from 0.05 to 0.04 and then to 0.03 micrometers leads to a decrease in the transition spring constant from $9x10^5$ to $8x10^5$ and then to $3x10^5$ N/m. This seems reasonable because less fillet radius results in less space within which maximum stress and maximum strain occur. Since what initiates pivoting is high degrees of strain in the fillet, less fillet radii cause pivoting mechanism more difficult to occur, so the cilium should be attached more loosely to the cell to be able to pivot easily around its base. Note that looser attachment equals lower spring constant.

Regarding validation of the model, we compared our results to those obtained by Rydholm et al. In addition to cilium length and width, all of the parameters listed in Table are those that Rydholm et al. used in their simulation and they are within the biological range. According to the plot shown in their paper, stress in ciliary microtubules is largest in the area around the base of the cilium with a magnitude of approximately 2000 to 3000 Pa for a cantilevered cilium of length 6 micrometers subject to a fluid flow of 0.044 Pa shear stress [9]. In our model, the maximum stress similarly occurs in the area around the base of the cilium but its magnitude is largely dependent on the spring constant of the thin elastic layer which attaches the cilium to the cell. Results of our simulation for a similar cilium with spring constant of 100000 N/m and different fillet radii subject to fluid flow of 0.04 are listed in Table 3 below.

Table 3 Maximum stress calculated for cilia of 6 μm length that are attached to the cell with elastic layers of 100000 N/m spring constants and subject to a flow of 0.04 Pa shear stress

Fillet radius (μm)	Maximum stress (Pa)
0.03	2540
0.04	2300
0.05	2140

It is clear that maximum stresses are within the range of 2000 to 3000 Pa that we expected. It is good to mention that in the model of Rydholm et al cilium consists of an elastic beam extending 6 μm into the extracellular space and 2 μm into the cell cytoplasm that is attached to the soft plasma membrane at the cell surface. In our model, however, the elastic beam does not extend into the cell cytoplasm, nor is it attached to any plasma membrane. Instead, it is attached to the cell surface through a thin elastic layer.

What further assures us of the validity of the model is the fact that our model is able to explain the two different modes of deflection of primary cilium. By examining relaxation behavior of deflected cilia from bend and relax experiments, Battle et al. found out that the relaxation curves could be better fit by a sum of two exponentials with two different time constants, which are related to two different modes of deflection, namely bending and pivoting [17]. Similarly, in our computational model, the presence of these two different modes of deflection are deduced from two different slopes of the curves discussed above. These modes, though observed and reported by Battle et al., was not simulated numerically in previous models.

In order to elicit adequate number of data and produce the graphs, simulations should be executed several times, which extensively increases computational costs of this study. That is why we used a two dimensional model in our simulations. We did not model the ciliary membrane either in order to further decrease computational costs. A three dimensional model with the modification presented in this study can be used in other simulations in order to produce more realistic results. For example, simulation of ciliary response to tensile strain that was studied by Mathieu et al. [16] can be carried out using this new model to investigate the probable modifications in the results. Calculating the delay in stress buildup in the ciliary membrane that was simulated by Rydholm et al. [9] is another subject for future study. This model can be used to see if this calculated time delay is changed as a result of the new type of attachment between cilium and cell.

Furthermore, this model could be used in analyzing the movement of motile cilia that are present in large numbers on such areas as the lining of trachea (windpipe), where they sweep mucus and dirt out of the lungs [24]. Since motile cilia move fluid by deforming in an organized and patterned matter, their bending or pivoting mode of deflection might have important consequences for their function.

4. Conclusion

The main question this study sought to answer was the consequences of a change in attachment of the primary cilium to the cell in terms of ciliary response to the fluid flow. Primary cilia as sensors of cells are able to sense the fluid flow surrounding the cells by being deflected in response to the shear stress exerted from the fluid. Although there is clear evidence that response of the cilium is in the forms of bending along its length and rotating around its base, to the best of our knowledge, there is no other numerical study that has simulated both modes of deflection. In our simulation, the primary cilium is attached to the cell surface through an infinitesimally thin layer with elastic properties. This layer, which is called spring

foundation, is a kind of boundary condition that applies to the bottom surface of the cilium and replaces the fixed boundary condition used in previous cantilevered models. The model was then solved using finite element methods and fluid-structure interaction techniques. This innovative model is able to explain the pivoting of the cilium around an imaginary hinge located at its base.

References:

[1] V. Singla, J. F. Reiter, The primary cilium as the cell's antenna: signaling at a sensory organelle, *science*, Vol. 313, No. 5787, pp. 629-633, 2006.

[2] P. Winyard, D. Jenkins, Putative roles of cilia in polycystic kidney disease, *Biochimica et Biophysica Acta (BBA)-Molecular Basis of Disease*, Vol. 1812, No. 10, pp. 1256-1262, 2011.

[3] D. A. Hoey, S. Tormey, S. Ramcharan, F. J. O'Brien, C. R. Jacobs, Primary Cilia-Mediated Mechanotransduction in Human Mesenchymal Stem Cells, *Stem cells*, Vol. 30, No. 11, pp. 2561-2570, 2012.

[4] P. Tummala, E. J. Arnsdorf, C. R. Jacobs, The role of primary cilia in mesenchymal stem cell differentiation: a pivotal switch in guiding lineage commitment, *Cellular and molecular bioengineering*, Vol. 3, No. 3, pp. 207-212, 2010.

[5] J. C. Bodle, C. D. Rubenstein, M. E. Phillips, S. H. Bernacki, J. Qi, A. J. Banes, E. G. Loboa, Primary cilia: the chemical antenna regulating human adipose-derived stem cell osteogenesis, 2013.

[6] A. D. Hanson, S. W. Marvel, S. H. Bernacki, A. J. Banes, J. van Aalst, E. G. Loboa, Osteogenic effects of rest inserted and continuous cyclic tensile strain on hASC lines with disparate osteodifferentiation capabilities, *Annals of biomedical engineering*, Vol. 37, No. 5, pp. 955-965, 2009.

[7] M. E. Wall, A. Rachlin, C. A. Otey, E. G. Loboa, Human adipose-derived adult stem cells upregulate palladin during osteogenesis and in response to cyclic tensile strain, *American Journal of Physiology-Cell Physiology*, Vol. 293, No. 5, pp. C1532-C1538, 2007.

[8] S. Diederichs, S. Böhm, A. Peterbauer, C. Kasper, T. Scheper, M. Van Griensven, Application of different strain regimes in two-dimensional and three-dimensional adipose tissue–derived stem cell cultures induces osteogenesis: Implications for bone tissue engineering, *Journal of Biomedical Materials Research Part A*, Vol. 94, No. 3, pp. 927-936, 2010.

[9] S. Rydholm, G. Zwartz, J. M. Kowalewski, P. Kamali-Zare, T. Frisk, H. Brismar, Mechanical properties of primary cilia regulate the response to fluid flow, *American Journal of Physiology-Renal Physiology*, Vol. 298, No. 5, pp. F1096-F1102, 2010.

[10] M. Fliegauf, T. Benzing, H. Omran, When cilia go bad: cilia defects and ciliopathies, *Nature reviews Molecular cell biology*, Vol. 8, No. 11, pp. 880-893, 2007.

[11] A. D. Güler, H. Lee, T. Iida, I. Shimizu, M. Tominaga, M. Caterina, Heat-evoked activation of the ion channel, TRPV4, *The Journal of neuroscience*, Vol. 22, No. 15, pp. 6408-6414, 2002.

[12] M. Köttgen, B. Buchholz, M. A. Garcia-Gonzalez, F. Kotsis, X. Fu, M. Doerken, C. Boehlke, D. Steffl, R. Tauber, T. Wegierski, TRPP2 and TRPV4 form a polymodal sensory channel complex, *The Journal of cell biology*, Vol. 182, No. 3, pp. 437-447, 2008.

[13] H. Praetorius, K. R. Spring, Bending the MDCK cell primary cilium increases intracellular calcium, *The Journal of membrane biology*, Vol. 184, No. 1, pp. 71-79, 2001.

[14] B. K. Yoder, X. Hou, L. M. Guay-Woodford, The polycystic kidney disease proteins, polycystin-1, polycystin-2, polaris, and cystin, are co-localized in renal cilia, *Journal of the American Society of Nephrology*, Vol. 13, No. 10, pp. 2508-2516, 2002.

[15] S. M. Nauli, F. J. Alenghat, Y. Luo, E. Williams, P. Vassilev, X. Li, A. E. Elia, W. Lu, E. M. Brown, S. J. Quinn, Polycystins 1 and 2 mediate mechanosensation in the primary cilium of kidney cells, *Nature genetics*, Vol. 33, No. 2, pp. 129-137, 2003.

[16] P. S. Mathieu, J. C. Bodle, E. G. Loboa, Primary cilium mechanotransduction of tensile strain in 3D culture: Finite element analyses of strain amplification caused by tensile strain applied to a primary cilium embedded in a collagen matrix, *Journal of biomechanics*, Vol. 47, No. 9, pp. 2211-2217, 2014.

[17] C. Battle, C. M. Ott, D. T. Burnette, J. Lippincott-Schwartz, C. F. Schmidt, Intracellular and extracellular forces drive primary cilia movement, *Proceedings of the National Academy of Sciences*, Vol. 112, No. 5, pp. 1410-1415, 2015.

[18] H. Khayyeri, S. Barreto, D. Lacroix, Primary cilia mechanics affects cell mechanosensation: A computational study, *Journal of theoretical biology*, Vol. 379, pp. 38-46, 2015.

[19] C. Multiphysics, 2014. Version 4.4. COMSOL, Inc., Burlington, MA, USA, pp. Fluid-Structure Interaction (fsi), Fluid Properties 1, Equation.

[20] C. Multiphysics, 2014. Version 4.4. COMSOL, Inc., Burlington, MA, USA, pp. Fluid-Structure Interaction (fsi), Fluid-Solid Interface Boundary 1, Equation.

[21] C. Multiphysics, 2014. Version 4.4. COMSOL, Inc., Burlington, MA, USA, pp. Fluid-Structure Interaction (fsi), Linear Elastic Material 1, Equation.

[22] C. Multiphysics, 2014. Version 4.4. COMSOL, Inc., Burlington, MA, USA, pp. Fluid-Structure Interaction (fsi), Fixed Constraint 1, Equation.

[23] C. Multiphysics, 2014. Version 4.4. COMSOL, Inc., Burlington, MA, USA, pp. Fluid-Structure Interaction (fsi), Spring Foundation 1, Equation.

[24] Y. Enuka, I. Hanukoglu, O. Edelheit, H. Vaknine, A. Hanukoglu, Epithelial sodium channels (ENaC) are uniformly distributed on motile cilia in the oviduct and the respiratory airways, *Histochemistry and cell biology*, Vol. 137, No. 3, pp. 339-353, 2012.